Chemistry−Structure−Simulation or Chemistry−Simulation−Structure Sequences? The Case of MIL-34, a New Porous Aluminophosphate

Thierry Loiseau,[†] Caroline Mellot-Draznieks,[†] Capucine Sassoye,[†] Stéphanie Girard,[†] Nathalie Guillou,[†] Clarisse Huguenard,[‡] Francis Taulelle,[‡] and Gérard Férey*,[†]

Contribution from the Institut Lavoisier, UMR CNRS 8637, Université de Versailles St. Quentin en Yvelines, 45, Avenue des Etats-Unis, 78035 Versailles Cedex, France and RMN et Chimie du Solide, UMR 7510, Université Louis Pasteur, 4, rue Blaise Pascal, 67070 Strasbourg, France

Received March 2, 2001

Abstract: A new aluminophosphate, MIL-34, is investigated from its as-synthesized structure to its calcined microporous form. Single-crystal X-ray diffraction measurements on the as-synthesized MIL-34 ($Al_4(PO_4)_4$-$OH{\cdot}C_4H_{10}N$, space group *P*-1, $a = 8.701(3)$ Å, $b = 9.210(3)$ Å, $c = 12.385(3)$ Å, $\alpha = 111.11(2)°$, $\beta = 101.42(2)°$, $\gamma = 102.08(2)°$, $V = 863.8(4)$ Å^3, $Z = 2$, $R = 3.8\%$) reveal a 3-D open framework where Al atoms are in both tetrahedral and trigonal bipyramidal coordinations. It contains a 2-D pore system defined by eight rings where channels along [100] cross channels running along [010] and [110]. CBuA molecules are trapped at their intersection. ^{27}Al, ^{31}P, and ^{1}H MAS NMR spectroscopies corroborate these structural features. Calcination treatments of a powder sample of the as-synthesized MIL-34 indicate its transformation into the related template-free structure that is stable up to 1000 °C. Lattice energy minimizations are then used in order to anticipate the crystal structure of the calcined MIL-34, starting with the knowledge of the as-synthesized structure exclusively. Energy minimizations predict a new regular zeotype structure ($AlPO_4$, space group *P*-1, $a = 8.706$ Å, $b = 8.749$ Å, $c = 12.768$ Å, $\alpha = 111.17°$, $\beta = 97.70°$, $\gamma = 105.14°$, $V = 846.75$ Å^3, $Z = 2$) together with a thermodynamic stability similar to that of existing zeotype AlPOs. Excellent agreement is observed between the diffraction pattern calculated from the predicted calcined MIL-34 and the experimental X-ray powder diffraction pattern of the calcined sample. Finally, the atomic coordinates and cell parameters of the calcined MIL-34 predicted from the simulations are used to perform the Rietveld refinement of the calcined sample powder pattern, further corroborated by ^{27}Al and ^{31}P NMR measurements. This unique combination of experiment and simulation approaches is an interesting and innovative strategy in materials sciences, where simulations articulate the prediction of a possible template-free framework from its as-synthesized templated form. This is especially valuable when straightforward characterizations of the solid of interest with conventional techniques are not easy to carry out.

Introduction

Following the extensive development of synthetic, microporous aluminosilicates, research has gradually shifted from zeolites toward the exploration of new families of three-dimensional frameworks. Since the discovery by Flanigen and co-workers of a new series of aluminophosphates (AlPOs) at the beginning of the 1980s,[1] there has been a continuously growing number of materials possessing open frameworks, with an unpreceded chemical diversification allowed by the exploration of metal substitutions.[2,3] In this context, the synthesis and characterization of AlPOs is still a very active research area. Indeed, a considerable number of AlPOs has been reported so far, with various architectures, for example, ranging from monodimensional chains systems[4] and layered compounds[5] to three-dimensional structures[6] including zeotype architectures. For example, the microporous AlPOs compounds include more than 40 different 3-D framework zeotypes.[7]

More generally, the ever-growing number of new inorganic structures is in part related to the extensive development of synthetic routes involving organic amines. The choice of the template molecules or structure-directing agents plays a central role in the synthesis of targeted open-framework architectures.

[†] Université de Versailles St. Quentin en Yvelines.

[‡] Université Louis Pasteur.

(1) Wilson, S. T.; Lok, B. M.; Messina, C. A.; Cannan, T. R.; Flanigen, E. M. *J. Am. Chem. Soc*. **1982**, *104*, 1146. Wilson, S. T.; Oak, S.; Lok, B. M.; Flanigen, E. M. U.S. Patent No. 4 310 440, 1982.

(2) Cheetham, A. K.; Férey, G.; Loiseau, T. *Angew. Chem., Int. Ed.* **1999**, *38*, 3268.

(3) Hartman, M.; Kevan, L. *Chem. Rev.* **1999**, *99*, 635.

(4) Oliver, S.; Kuperman, A.; Lough, A.; Ozin, G. A. *Inorg. Chem.* **1996**, *35*, 6373. Chippindale, A. M.; Turner, C. *J. Solid State Chem.* **1997**, *128*, 318.

(5) Riou, D.; Loiseau, T.; Férey, G. *J. Solid State Chem.* **1993**, *102*, 4. Kongshaug, K. O.; Fjellvag, H.; Lillerud, K. P. *Microporous Mesoporous Mater.* **2000**, *38*, 311. Yuan, H.-M.; Chen, J.-S.; Shi, Z.; Chen, W.; Wang, Y.; Zhang, P.; Yu, J.-H.; Xu, R.-R. *J. Chem. Soc., Dalton. Trans.* **2000**, 1981. Chippindale, A. M.; Walton, R. I. *J. Solid State Chem.* **1999**, *145*, 731.

(6) Davis, M. E.; Saldarriaga, C.; Montes, C.; Garces, J. M.; Crowder, C. *Nature* **1988**, *331*, 698. Jones, R. H.; Thomas, J. M.; Chen, J.; Xu, R.; Huo, Q.; Li, S.; Ma, Z.; Chippindale, A. M. *J. Solid State Chem.* **1993**, *102*, 204. Férey, G.; Loiseau, T.; Lacorre, P.; Taulelle, F. *J. Solid State Chem.* **1993**, *105*, 179. Kongshaug, K. O.; Fjellvag, H.; Klewe, B.; Lillerud, K. P. *Microporous Mesoporous Mater*. **2000**, *39*, 333. Kirchner, R. M.; Grosse-Kunstleve, R. W.; Pluth, J. J.; Wilson, S. T.; Broach, R. W.; Smith, J. V. *Microporous Mesoporous Mater.* **2000**, *39*, 319.

(7) Meier, W. M.; Olson, D. H.; Baerlocher, C. *Atlas of Zeolite Structure Types*, 4th rev. ed.; Elsevier: London, 1996.

10.1021/ja010575b CCC: $20.00
Published on Web 09/06/2001

They are incorporated in the final structure, acting as compensating charges or allowing the production of micropores with tailored size and shape. Also, the production of the related template-free open-framework materials is of crucial interest. In a number of cases, metalloaluminophosphates for example, the nonframework species may be removed from the structure, leaving behind an open framework with interesting adsorption or catalytic properties.[8] However, the removal of the template is often a critical step, and the production of the related stable open-framework structure cannot be easily anticipated. To the best of our knowledge, there has been no systematic attempt to rationalize the structural and energetic relationships between as-synthesized templated structures and their related template-free forms.

In the past decade, the use of computational approaches to provide valuable information concerning the structures and energetics of microporous materials has grown extensively.[9] Recently, we have carried out investigations[10] on the as-synthesized templated aluminophosphate, $AlPO_4$-14,[11,12] to explore whether simulations could anticipate the stability and structure of its template-free form. Interestingly, the crystal structure of $AlPO_4$-14 in its calcined form was predicted[10] in close agreement with the experimental synchrotron powder diffraction analysis,[11] by using lattice energy minimization techniques and appropriate interatomic potentials. Such a study highlighted the possibility of using computational approaches for exploring thermodynamic stabilities of as-synthesized open-framework structures upon template extraction.

In this work, we present the synthesis and characterization of a new 3-D open-framework aluminophosphate, MIL-34 ($Al_4(PO_4)_4OH{\cdot}C_4H_{10}N$), in both its as-synthesized form in the presence of cyclobutylamine and its calcined microporous form. We characterize this new AlPO in its as-synthesized form using single-crystal diffraction together with ^1H, ^{13}C, ^{27}Al, and ^{31}P NMR spectroscopies. We then investigate its thermal stability upon calcination treatment. In view of experimental results, we anticipate the crystal structure of the related open-framework template-free material, using energy minimizations and appropriate interatomic potentials for describing the inorganic framework. Our aim is to get useful and reliable insights into the lattice energy and structure of the calcined MIL-34 that are difficult to access experimentally. It appears that such an experiment/simulation combination is highly valuable in these typical cases where obtaining a single crystal or a pure powder of the calcined phase suitable for further characterizations, i.e., structure determination, is obviously a difficult task.

Experimental Section

Synthesis. The synthesis of MIL-34, namely $Al_4(PO_4)_4OH$, $C_4H_{10}N$, was carried out under mild hydrothermal conditions using aluminum hydroxide ($Al(OH)_3$, Prolabo, 65% Al_2O_3), phosphoric acid (H_3PO_4, 85% Prolabo), cyclobutylamine ($C_4H_{10}N$, >98% Fluka, noted CBuA), and desionized water. A typical reaction contained these components in the following molar ratio: 1 $Al(OH)_3$:1 H_3PO_4:1 CBuA:80 H_2O. The reaction was done at 180 °C in a 23 mL Teflon-lined stainless steel Parr digestion bomb under autogenous pressure for 10 days. After being filtered off and washed with deionized water, the resulting white product was dried at room temperature and characterized by single-crystal X-ray diffraction.

Table 1. Single Crystal Data and Structure Refinement of the As-Synthesized MIL-34

formula	$Al_4(PO_4)_4OH{\cdot}C_4H_{10}N$
crystal size (μm)	240 × 160 × 120
data collection temperature (K)	296
wavelength (Å)	0.71073
space group	*P*-1
a (Å)	8.701(3)
b (Å)	9.210(3)
c (Å)	12.385(3)
α (deg)	111.11(2)
β (deg)	101.42(2)
γ (deg)	102.08(2)
volume (Å^3)	863.8(4)
Z	2
density$_{calcd}$ (g·cm^{-3})	2.218
Δ2*θ* data collection (deg)	1.85−29.80
limiting indices	$-12 \le h \le 12$, $-12 \le k \le 6$, $-16 \le l \le 17$
absorption coefficient (mm^{-1})	0.736
F(000)	580
reflections collected	6151
independent reflections	4336 [*R*(int) = 0.0161]
refinement method	full-matrix least-squares on F^2
no. of parameters	273
GOF on F^2	0.956
final *R* indices (for $I > 2\sigma(I)$)	$R_1{}^a = 0.0385$, w$R_2{}^b = 0.0980$
R indices (all data)	$R_1{}^a = 0.0455$, w$R_2{}^b = 0.1030$
extinction coefficient	0.0120(13)
residual electron density (min,max) (e·Å^{-3})	−1.109; 1.351

$^a R_1 = \sum||F_o| - |F_c||/\sum|F_o|$. ^{b} w$R_2 = [\sum[w(F_o^2 - F_c^2)^2]/\sum[w(F_o^2)^2]]^{1/2}$.

Single-Crystal X-ray Crystallography. A colorless single crystal of the as-synthesized MIL-34, size 240 μm × 160 μm × 120 μm, was carefully selected under a polarizing optical microscope and mounted on a glass fiber. The intensity data were recorded on a Siemens SMART three-circle diffractometer equipped with a CCD bidimensional detector (Mo Kα radiation) operating at 50 kV and 40 mA. The crystal-to-detector distance was 45 mm, allowing for data collection up to 60° (2*θ*), and slightly more than one hemisphere of data was recorded. The frames were collected with a scan width of 0.3° in *ω* and an exposure time of 30 s. Details of the data collection are given in Table 1. The structure was solved by direct methods in the centric space group *P*-1 and refined by full-matrix least squares using the SHELXTL package.[13] The difference Fourier syntheses revealed all the non-hydrogen atoms (Al, P, O, C, N), and the H atoms of the CBuA molecules were placed with geometrical restraints in the riding mode.

Magic Angle Spinning (MAS) NMR. ^{31}P, ^{27}Al, ^1H, and $^{13}C\{^1H\}$ CP MAS experiments have been conducted on the as-synthesized MIL-34. The calcined phase has been studied by ^{27}Al (MAS, MQMAS) and ^{31}P NMR. The spectrometers used were Bruker DSX 500 and DMX 800 with MAS probes with rotors of 4 or 2.5 mm in diameter. The experimental conditions of acquisitions are given in Table 2. In the case of aluminum, the field of 18.8 T helped to resolve the inequivalent sites. For the other nuclei a field of 11.7 T was used. Fast rotation between 10 and 22 kHz allowed us to get better resolution of inequivalent sites and better quantification of sites.

Thermogravimetry and Thermodiffraction. The thermal analysis (TGA/DTA) of the as-synthesized templated MIL-34 was carried out on a TA instrument type 2050 thermoanalyzer under oxygen gas flow

(8) Lok, B. M.; Messian, C. A.; Patton, R. L.; Gajek, R. T.; Cannan, T. R.; Flanigen, E. M. *J. Am. Chem. Soc.* **1984**, *106*, 6092. Sierra de Saldarriaga, L.; Saldarriaga, C.; Davis, M. E. *J. Am. Chem. Soc.* **1987**, *109*, 2686.

(9) *Computer Modelling in Inorganic Crystallography*; Catlow, C. R. A., Ed.; Academic Press: London, 1997.

(10) Girard, S.; Mellot-Draznieks, C.; Gale, J. D.; Férey G. *Chem. Commun.* **2000**, 1161.

(11) Zibrowius, B.; Lohse, U.; Szulzewsky, K.; Fichtner-Schmittler, H.; Pritzkow, W.; Richter-Mendau, J. *Stud. Surf. Sci. Catal.* **1991**, *65*, 549.

(12) Broach, R. W.; Wilson, S. T.; Kirchner, R. M. In *Proceedings of the 12th International Zeolite Conference*; Treacy, M. M. J., Marcus, B. K., Bisher, M. E., Higgins, J. B., Eds.; Materials Research Society: Warrendale, PA, 1999; p 1715.

(13) Sheldrick, G. M.; SHELXTL Version 503, Software Package for the Crystal Structure Determination, Siemens Analytical X-ray Instruments Inc., Madison, WI, 1994.

Table 2. NMR Experimental Acquisition Conditions

	nucleus			
	^{1}H	^{13}C	^{27}Al	^{31}P
spectrometer	DSX 500	DSX 500	AMX 800	DSX 500
probehead	H-X 4 mm MAS	H-X 4 mm MAS	H-X 2.5 mm MAS	H-X 4 mm MAS
Larmor frequency (MHz)	500.030	^{13}C 125.732 ^{1}H 500.030	208.493	202.416
spinning speed (kHz)	18	10	22	18
pulse sequence	single pulse	CPMAS	single pulse	single pulse
radio frequency field	31	^{13}C 50/^{1}H 40	55	44
(kHz)/90° (μs)	8	6.25	4.4	5.7
pulse length (μs)	4	6.25/contact 10 ms	1	4
spectral width (kHz)	60	12	100	60
recycle time (s)	10	20	1	60
accumulated scans	8	1024	128	128
secondary reference	adamantane (1.8 ppm)	adamatane (29.4 and 38.4 ppm)		
reference (0 ppm)	TMS	TMS	$Al(NO_3)_3/H_2O$ 1 M	H_3PO_4/85% H_2O

with a heating rate of 2 °C·min^{-1}. The thermodiffractometry was performed under vacuum (10^{-3} Torr) in a high-temperature device (Anton Paar HTK16) of a Siemens D5000 X-ray powder diffractometer ($\theta-\theta$) mode using Co Kα radiation ($\lambda = 1.7903$ Å), equipped with a M Braun linear position-sensitive detector (PSD). The patterns were collected up to 1000 °C every 40 °C, with the temperature increasing at a rate of 2 °C·min^{-1}.

Specific Areas Study. The BET surface area analysis was performed on a Micrometrics ASP200 porosimeter.

Computer Simulations. Energy minimizations were used with the aim of anticipating both the stability and the crystal structure of the calcined MIL-34, i.e., in the absence of the CBuA structure-directing agent, starting from the knowledge of the as-synthesized structure only. The single crystal data of the as-synthesized templated MIL-34 structure in this work were used directly as a starting model and modified prior to energy minimization as follows: atoms that are presumed to evacuate upon calcination, i.e., hydroxy groups and CBuA molecules, were removed from the structure file, leaving behind a neutral open-framework structure, namely, $AlPO_4$. This model structure was then submitted to constant pressure (i.e., allowing both cell parameters and fractional coordinates to relax) minimization in space group *P*-1.

Calculations were carried out using appropriate interatomic potentials developed by Gale and Henson for AlPOs[14] and the lattice energy minimization code GULP.[15] The robustness of their formal charge shell model force field has been demonstrated through the accurate reproduction of experimentally determined structures of AlPOs[16] together with estimations of their relative framework stabilities that are consistent with thermodynamic data.[17]

Interactions between two ions, *i* and *j*, are described by a Buckingham potential combined with a Coulombic term to describe the electrostatic interactions:

$$E_{ij} = A_{ij}\exp(-r_{ij}/\rho_{ij}) - C_{ij}r_{ij}^{-6} + q_iq_j/r_{ij} \quad (1)$$

where q_i and q_j refer to the charges of the ions, and A_{ij}, ρ_{ij}, and C_{ij} are short-range potential parameters. This energy was computed with a short-range summation taken up to a cutoff radius of 16 Å and an Ewald summation for the electrostatic term. Ionic polarizability of the oxygen atoms is incorporated using the shell model of Dick and Overhauser[18] in which an ion is represented by a core and a shell coupled by a harmonic spring:

$$E_{\text{core-shell}} = {}^1/_2k(r_{\text{core-shell}})^2 \quad (2)$$

The inclusion of three-body forces acting on O−Al−O angles was also considered in the form of a harmonic angle-bending potential, where θ_o is the equilibrium tetrahedral bond angle at the pivot atom *j*:

$$E_{ijk} = {}^1/_2K_{ijk}(\theta_{ijk} - \theta_o)^2 \quad (3)$$

Force field parameters are those reported in ref 13.

Rietveld Refinement of Calcined MIL-34. The X-ray powder diffraction data of the calcined MIL-34 were collected using Cu Kα radiation ($\lambda = 1.5418$ Å) on a Siemens D5005 diffractometer equipped with an HTK 1200 temperature device. MIL-34 was heated in situ at 100 °C for 5 h under vacuum and then at 600 °C for 73 h. The powder diffraction pattern was then scanned at 120 °C over the 6−60° (2θ) angular range with a counting time of 20 s·step^{-1}. The pattern indexing was performed from the 20 first lines using DICVOL91,[19] with an absolute error on peak positions of 0.03° (2θ). The atomic coordinates predicted in the simulation section were used as a starting model in our Rietveld refinement using the FullProf.98[20] program integrated in WinPLOTR software.[21] Unit cell and instrumental parameters were allowed to vary during the refinement process. One region of the powder pattern, corresponding to the highest line of the main impurity, was excluded. The final Rietveld refinement was carried out in the angular range 6−60° (2θ) using 493 reflections.

Results and Discussion

Crystal Structure of the As-Synthesized MIL-34. The final refinement including the atomic positions for all atoms and anisotropic thermal parameters for all non-hydrogen atoms and isotropic thermal parameters for all hydrogen atoms converged to $R_1(F) = 0.0385$ and $wR_2(F^2) = 0.0980$ for 4336 reflections ($I > 2\sigma(I)$). Final atomic coordinates and temperature factors are given in Table 3. Selected bond distances and angles are given as Supporting Information.

The crystal structure of the as-synthesized MIL-34 is shown in Figure 1. It consists of a 3-D framework made of PO_4 tetrahedra connected with AlO_4 tetrahedra and $AlO_4(OH)$ trigonal bipyramids, which encloses CBuA species. All the polyhedra are connected to each other by corner sharing. The four inequivalent P atoms are tetrahedrally coordinated with typical average P−O distances (1.525 Å) and O−P−O angles (109.44°) as expected from the AlPO-*n* series. While two of the four inequivalent Al atoms, Al(1) and Al(3), are in regular tetrahedral coordination ($\langle Al_{1,3}-O\rangle = 1.73$ Å and $\langle O-Al_{1,3}-O\rangle = 109.45°$), the two remaining ones, Al(2) and Al(4), are in

(14) Gale, J. D.; Henson, N. J. *J. Chem. Soc., Faraday Trans.* **1994**, *90*, 3175.
(15) Gale, J. D. *J. Chem. Soc., Faraday Trans.* **1997**, *93*, 629.
(16) Henson, N. J.; Cheetham, A. K.; Gale, J. D. *Chem. Mater.* **1996**, *8*, 664.
(17) Navrotsky, A.; Petrovic, I.; Hu, Y.; Chen, C.-Y.; Davis, M. E. *Micro. Mater.* **1995**, *4*, 95.
(18) Dick, B. G.; Overhauser, A. W. *Phys. Rev.* **1958**, *112*, 90.
(19) Boultif, A.; Louër, D. *J. Appl. Crystallogr.* **1991**, *24*, 987.
(20) *FullProf.98 and WinPLOTR: New Windows 95/NT Applications for Diffraction.* Rodríguez-Carvajal, J., Roisnel, T.; Newsletter No. 20 (May−August) Summer 1998.
(21) Roisnel, T.; Rodriguez-Carvajal, J. WinPLOTR: a Windows tool for powder diffraction patterns analysis. *Materials Science Forum*, Proceedings of the European Powder Diffraction Conference (EPDIC 7), in press.

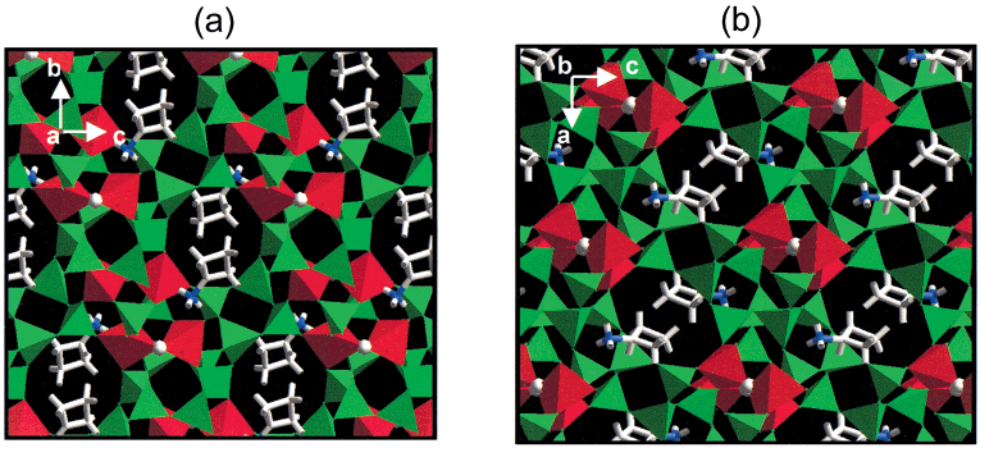

Figure 1. Polyhedral representation of the as-synthesized MIL-34 **(a)** along [100] and **(b)** along [010]. All AlO_4 and PO_4 tetrahedra are represented in green, while bipyramids corresponding to aluminum atoms in five-fold coordination are represented in red. For clarity, only oxygen atoms belonging to hydroxy groups are shown (white balls), and template molecules are represented with sticks.

Table 3. Final Atomic Coordinates and Equalized Temperature Factors (ESDs in Parentheses) for the As-Synthesized Templated MIL-34 Structure

atom	x	y	z	U(eq) (Å^2 × 10^3)
Al(1)	−0.6985(1)	−0.2096(1)	−0.3759(1)	9(1)
Al(2)	−0.3506(1)	−0.2177(1)	−0.1443(1)	9(1)
Al(3)	−0.9802(1)	−0.6694(1)	−0.0572(1)	9(1)
Al(4)	−0.5051(1)	−0.2067(1)	−0.1462(1)	9(1)
P(1)	−0.4010(1)	−0.5160(1)	−0.1989(1)	9(1)
P(2)	−0.4429(1)	−0.0549(1)	−0.3433(1)	9(1)
P(3)	−0.2206(1)	−0.0517(1)	−0.0678(1)	9(1)
P(4)	−1.0363(1)	−0.3432(1)	−0.1807(1)	9(1)
O(1)	−0.3268(2)	−0.1599(2)	−0.4723(2)	15(1)
O(2)	−0.4836(2)	−0.1643(2)	−0.2835(2)	14(1)
O(3)	−0.9094(2)	−0.2594(3)	−0.3065(2)	16(1)
O(4)	−0.4884(2)	−0.2519(2)	−0.0016(2)	12(1)
O(5)	−0.3633(2)	−0.0652(2)	−0.2768(2)	16(1)
O(6)	−0.4915(2)	−0.4050(2)	−0.2300(2)	15(1)
O(7)	−0.4879(2)	−0.6138(2)	−0.1422(2)	15(1)
O(8)	−0.6053(2)	−0.0399(2)	−0.3540(2)	16(1)
O(9)	−0.3766(3)	−0.6288(2)	−0.3160(2)	18(1)
O(10)	−1.0715(3)	−0.5284(2)	−0.1322(2)	19(1)
O(11)	−0.2305(2)	−0.4082(2)	−0.1097(2)	19(1)
O(12)	−1.1945(2)	−0.3043(2)	−0.1870(2)	14(1)
O(13)	−0.3072(2)	−0.1652(2)	−0.1347(2)	15(1)
O(14)	−0.0496(2)	−0.1557(2)	−0.0787(2)	12(1)
O(15)	−0.1905(2)	−0.656(2)	−0.1242(2)	12(1)
O(16)	−0.3164(2)	0.0418(2)	−0.0671(2)	14(1)
O(17)	−0.9580(2)	−0.2831(2)	−0.0974(2)	16(1)
N	−0.1522(3)	−0.0946(4)	−0.2660(3)	26(1)
C(1)	−0.0796(10)	−0.3433(8)	-0.3932(6)	84(2)
C(2)	−0.8470(9)	−0.6044(9)	−0.4716(5)	79(2)
C(3)	−0.1566(14)	−0.2202(12)	−0.3747(6)	141(5)
C(4)	−0.2123(19)	−0.2525(16)	−0.4918(7)	226(9)

five-fold coordination with a trigonal bipyramid geometry. The special environment of the two latter aluminum atoms comes from an additional oxygen, O(4), which links both Al atoms as shown by bond valence calculations, which leads to significant distortions of both polyhedra AlO_4OH (Al−O within 1.77−1.97 Å).

Figure 2a shows the topology of the MIL-34 network. Topologically, the MIL-34 structure may be described by using a building unit derived from the double six-membered ring entity (D6R) and comprising six P centers and six Al centers (Figure 2b). The occurrence of an Al−O−Al bonding induces a distortion in one of the six-membered rings of the D6R unit and leads to an Al−O−P linkage interruption (d_{Al-P} = 4.94 Å). These open-D6R units are linked to each other through the four-membered-ring faces located in cis position, generating cis infinite chains of open-D6R units along [001] (Figure 2c, left). A situation similar to that of MIL-34 also occurs in the structures $AlPO_4$-HDA[22] and $Al_2(PO_4)(HPO_4)(C_2O_4)(N_2C_4H_{12})(H_2O)$[23] (Figure 2c, middle), which are both based on columns of face-sharing D6R species. However, in the latter compounds, the connection of the D6R units is ensured via two opposite four-membered-ring faces (trans file of D6Rs).

In the (110) plane, the chains are connected together by forming sheets of six-membered rings alternating with eight-membered rings (Figure 2a). These layers are linked perpendicular to [001] via all the free remaining corners, leading to the 3-D framework.

The open-framework contains a two-dimensional pore system defined by eight-membered rings. The channels along [100] cross channels running along [010] and [110]. Two CBuA template molecules are trapped at the intersection of the tunnels, encapsulated in $4^86^28^6$ cages (Figure 2d). Each CBuA molecule is protonated and balances the charge of a hydroxy group. In addition, hydrogen bonds with the framework appear to be optimized since the ammonium groups point toward the six-membered ring with N···O distances ranging from 2.88 to 3.05 Å. N atoms interact preferentially via hydrogen bonds, with the oxygen atoms belonging to the coordination sphere of P(2) and P(3).

MAS NMR Studies of the As-Synthesized MIL-34. The ^{1}H MAS NMR spectrum (Figure 3, left) indicates three distinct lines at 2.3, 4.0, and 6.8 ppm in a 0.674:0.08:0.246 ratio. They can easily be assigned to H atoms belonging respectively to (OH and CH_2), CH, and NH_3 groups for which we would get a theoretical ratio of 0.636:0.09:0.273 (i.e., (7/11)/(1/11)/(3/11)). The chemical shift of 2.3 matches C(1,2,4)H_2 as well as the bridging O*H* between two aluminum atoms. N*H* is found at 6.8 ppm and C(3)(N)*H* at 4.0 ppm. The ^{13}C CPMAS experiment (Figure 3, right) leads to three distinct lines at 16.5, 29.3, and 46.6 ppm in a 0.25:0.51:0.24 ratio. The assignment is again straightforward, with C3 attached to nitrogen resonating at 46.6 ppm, and C1,4 not resolved at 29.3 ppm and C2 at 16.5 ppm. With this assignment the proper ratio of 1:2:1 (or 0.25:0.50:0.25) is found. Four inequivalent phosphorus atoms are observed

(22) Yu, J.; Sugiyama, K.; Zheng, S.; Qiu, S.; Chen, J.; Xu, R.; Sakamoto, Y.; Terasaki, O.; Hiraga, K.; Light, M.; Hursthouse, M. B.; Thomas, J. M. *Chem. Mater*. **1998**, *10*, 1208.

(23) Kedarnath, K.; Choudhury, A.; Natarajan S. *J. Solid State Chem.* **2000**, *150*, 324−329.

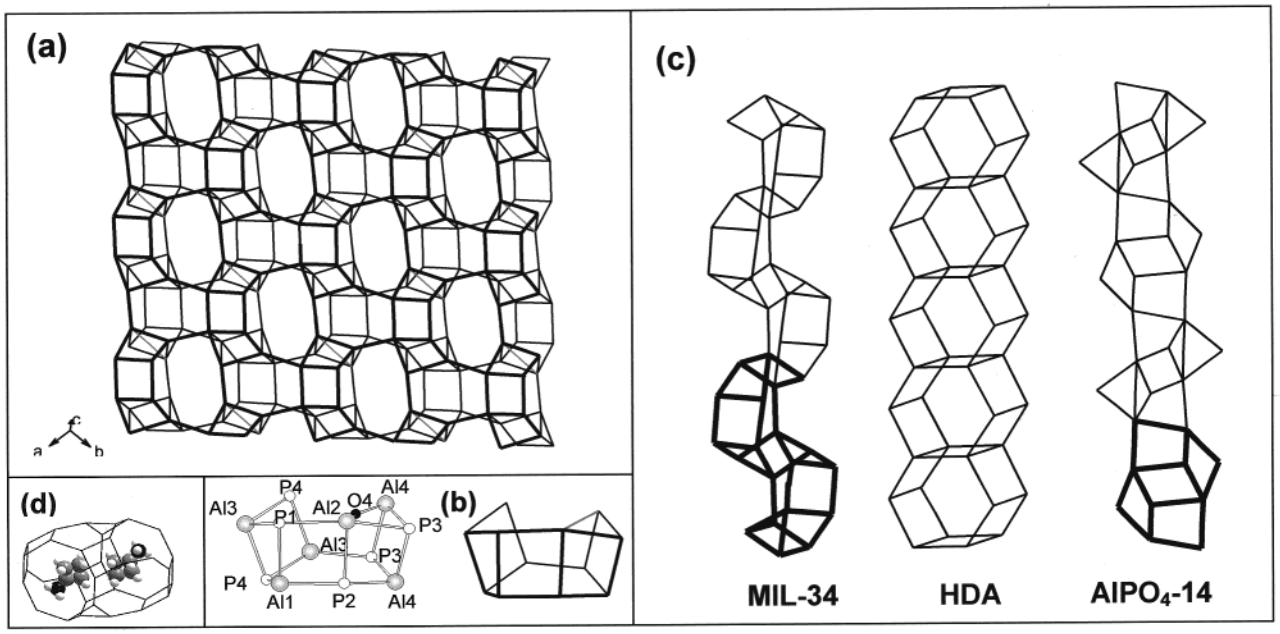

Figure 2. As-synthesized MIL-34 structure and selected comparison with other AlPOs. **(a)** Framework topology of MIL-34 in the [110] plane. **(b)** Open-D6R units extracted from MIL-34. **(c)** Description of chains connection in MIL-34 (left), $AlPO_4$-HDA, and $Al_2(PO_4)(HPO_4)(C_2O_4)(N_2C_4H_{12})(H_2O)$ (middle) and $AlPO_4$-14 (right). **(d)** CBuA template molecules are trapped in $4^86^28^6$ cages in MIL-34. Al−OH−Al linkages are shown in gray, except for (c), where Al−OH−Al linkages are not shown.

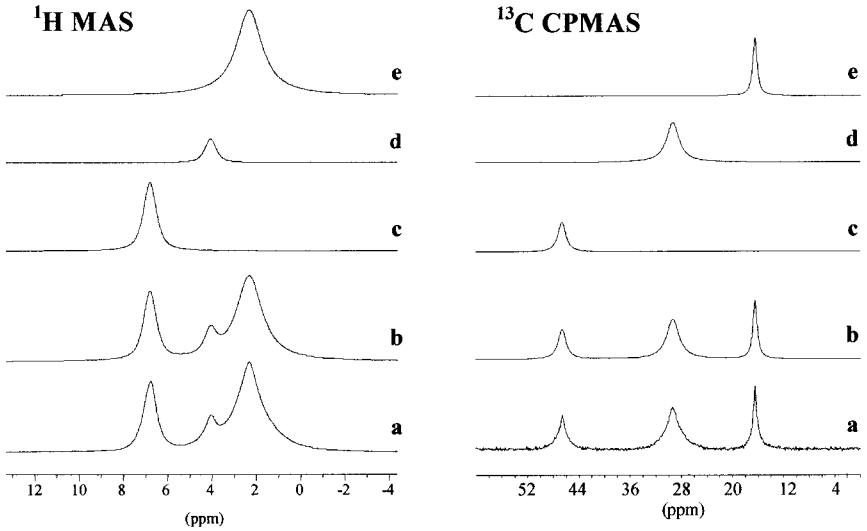

Figure 3. Left: ^{1}H MAS NMR. (a) Experimental spectrum, Winfit simulated. (b) Total sum of components. (c) N*H* site at 6.8 ppm. (d) C(N)*H* site at 4.0 ppm (e) CH_2 and O*H* sites at 2.3 ppm. Right: ^{13}C {^{1}H} CPMAS NMR. (a) Experimental spectrum, Winfit simulated. (b) Sum of components. (c) C(3)HNH_3 component at 46.6 ppm. (d) C(1,4)H_2 at 29.3 ppm. (e) C(2)H_2 at 16.5 ppm.

in the ^{31}P MAS NMR at −16.3, −22.3, −27.4, and −29.1 ppm (Figure 4, left). They follow a usual linear relationship between the mean P−O distance and the isotropic chemical shift. If phosphorus atoms are ranked by their distances, P3−P2−P4−P1 with 1.5272−1.5252−1.5245−1.5230 Å, then the relation with chemical shifts ranked by decreasing chemical shift with decreasing distance leads to $\delta_{iso} = 1.5232\ \text{Å} + (2.9 \times 10^{-4})\delta_{iso}$ (ppm).[24] This crude method is usually enough to assign sites correctly. If a totally unambiguous site assignment were mandatory, one would have to run a double-quantum experiment that analyzes the phosphorus sublattice topology and allows very accurate assignment without empirical knowledge.[25] Therefore, the inequivalent phosphorus sites can be assigned accordingly, P3−P2−P4−P1 with the phosphorus resonating at −16.3, −22.3, −27.4, and −29.1 ppm. For aluminum, Figure 4 (right) displays its MAS spectrum expanded to its central region. An inset emphasizes the first rotation bands of the external transitions. The first external transitions are clearly visible, while the second external transitions are hardly visible. Four sites are well resolved on the external transitions. This allows us to consider the central transitions and to recognize four second-order quadrupolar patterns. Two of them are resolved at 44 and 48 ppm, though two others at 14 and 18 ppm are overlapping. An STMAS experiment[26] has allowed us to separate clearly these two sites and to analyze them. The MAS spectrum can

(24) Campomar, V. RMN en Rotation à l'Angle Magique du ^{31}P. Application à l'étude de quelques phosphates. Ph.D. Dissertation, University Pierre and Marie Curie, Paris, 1990.

(25) Munch, V.; Taulelle, F.; Loiseau, T.; Ferey, G.; Cheetham, A. K.; Weigel, S.; Stucky, G. D. *Magn. Reson. Chem.* **1999**, *37*, 100.

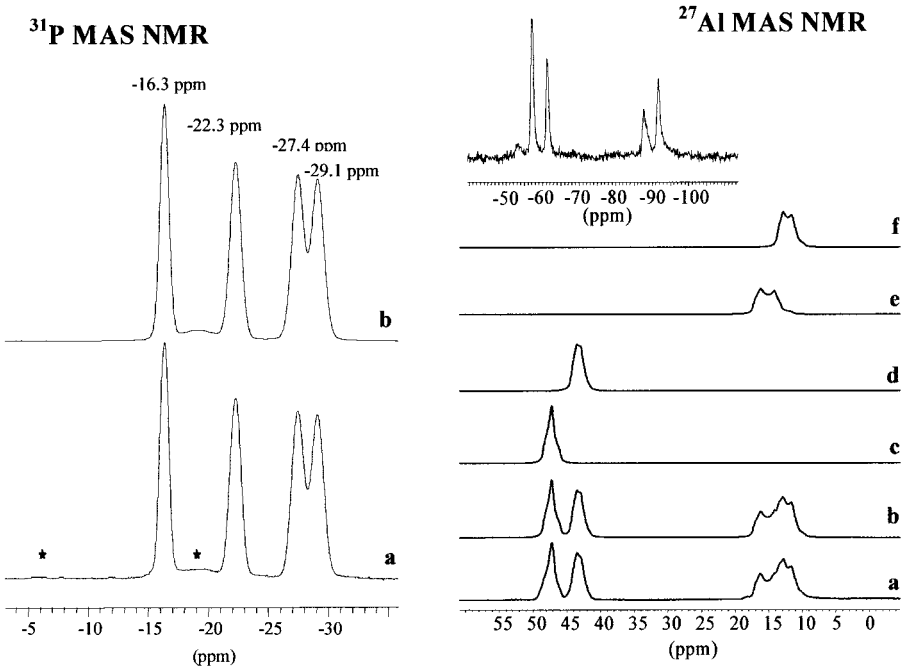

Figure 4. Left: ^{31}P MAS NMR. (a) Experimental spectrum. (b) Winfit simulated sum of components at −16.3, −22.3, −27.4, and −29.1 assigned respectively to P3, P2, P4, and P1. Right: ^{27}Al MAS NMR. (a) Experimental spectrum expanded to central transitions; Winfit simulated. (b) Sum of components. (c) $\delta_{iso} = 48.4$ ppm, $\nu_Q = 380$ kHz ($C_Q = 2530$ kHz), $\eta_Q = 1$, integral = 24%. (d) $\delta_{iso} = 44.3$ ppm, $\nu_Q = 425$ kHz ($C_Q = 2830$ kHz), $\eta_Q = 0.50$, integral = 25%. (e) $\delta_{iso} = 17.7$ ppm, $\nu_Q = 640$ kHz ($C_Q = 4267$ kHz), $\eta_Q = 0.30$, integral = 25%. (f) $\delta_{iso} = 13.95$ ppm, $\nu_Q = 530$ kHz ($C_Q = 3540$ kHz), $\eta_Q = 0.35$, integral = 26%. (g) External transitions of first spinning sidebands pattern; four resolved components are present.

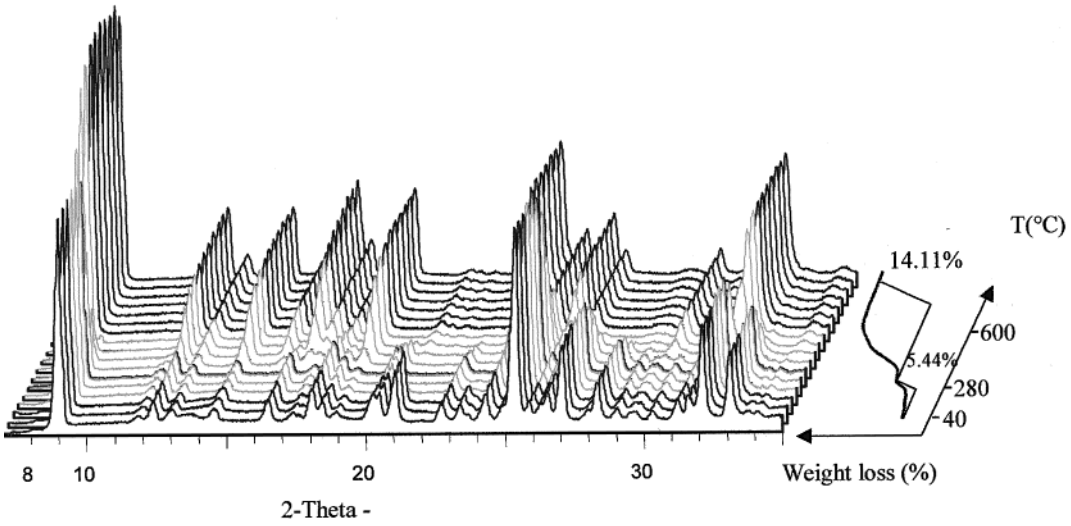

Figure 5. Thermal behavior of the as-synthesized MIL-34: 3-D representation (left) of high-temperature powder X-ray data for MIL-34 within the 40−1000 °C temperature range under vacuum (10^{-3} Torr), shown together with the thermogravimetry analysis (right) under oxygen gas flow with a heating rate of 2 °C min^{-1}.

therefore be described by a superposition of four sites with two in the region of four-coordinated sites and two in the region of five-coordination. The aluminum chemical shift is a function of its coordination state but depends also on the second-sphere neighbor. For aluminophosphates the four-coordination range is around 40 ppm, the six-coordination around −20 ppm, and the expected five-coordination around 10 ppm. However in the actual sample, four Al−O bonds are Al−O−P bonds, and the fifth is an Al−OH−Al bond. So we can expect a chemical shift 4−5 ppm higher than with only Al−O−P bonds. This is the case with two isotropic chemical shifts at 14 and 18 ppm. The area ratio indicates a 1:1:1:1 site population in agreement with the single-crystal structure. The different nuclei observed by NMR on the powder indicate a clear agreement between the inequivalent sites seen by NMR and the single-crystal structure determination.

Phase Transformation: Thermogravimetry and Thermodiffractometry. The thermogravimetry curve (Figure 5) shows two successive steps between 25 and 1050 °C. The first weight loss (5.44%) below 280 °C was assigned to the evacuation of a small amount of water molecules that are disorderedly adsorbed within the structure, inducing no significant changes in the corresponding diffraction patterns. Indeed, this loss was not assigned to the departure of the hydroxyl groups since the

(26) Huguenard, C.; Gan, Z.; Steurnagel, S.; Loiseau, T.; Férey, G.; Taulelle, F., to be submitted, 2001.

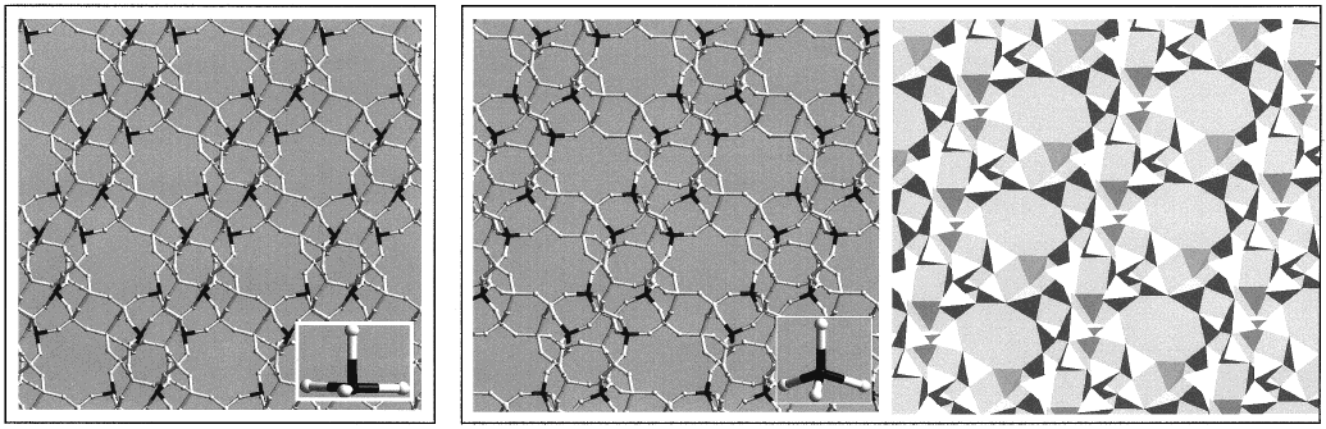

Figure 6. Left: Initial model for calcined MIL-34 used in our calculations and constructed from its as-synthesized form, removing the templating agent and bridging hydroxy groups. This model structure is left with Al atoms in highly distorted tetrahedral environments. Right: Predicted structure for calcined MIL-34 from constant pressure energy minimization of the initial model showing the regular tetrahedral environment of Al atoms, in its tetrahedral and stick representations viewed down the [010] direction. Its zeotype structure emanates from the corner-sharing connection and strict alternation of AlO_4 and PO_4 tetrahedra into a microporous 3-D framework.

diffraction patterns of MIL-34 were identical up to 280 °C. The second weight loss (14.11%) occurred between 280 and 600 °C and was attributed to the decomposition of CBuA molecules combined with a dehydroxylation reaction, which is consistent with the amount of template and hydroxy groups calculated from the crystal structure determination (calcd, 15.42%). Both thermodiffractometry (Figure 5) and TGA confirm that decomposition of template molecules and dehydroxylation occur at the same time.

Indeed, the appearance of a new pattern at high temperature, observed up to 1000 °C, with features distinctly different from those of the original as-synthesized structure, reveals the transformation of the as-synthesized MIL-34 structure into a new crystalline phase. This resulting material is obviously structurally related to the as-synthesized original structure and will be referred to as the calcined MIL-34 structure in the following sections.

Calcined MIL-34: Anticipation of the Structure by Simulations. Previous lattice energy minimizations performed by us have clearly shown[10] that a computational approach could be used for anticipating the framework stability and crystal structure of an open-framework aluminophosphate upon template extraction: the calcined form of $AlPO_4$-14 was predicted starting from the knowledge of the as-synthesized structure only, simply by virtually eliminating the template molecules, the bridging hydroxy groups, and water molecules and using appropriate interatomic potentials[13] for describing interactions within the inorganic framework.

Interestingly, the as-synthesized MIL-34 structure shows some similarities with that of $AlPO_4$-14.[11] Both structures have the same framework chemical composition and space group (*P*-1), with the same number of inequivalent Al and P atoms. The two compounds also have close cell volumes and a similar 2-D pore system made of eight-membered rings. $AlPO_4$-14 can be described with chains made of opposed edge-sharing open double cubes (Figure 2c, right), while MIL-34 is built of opposed face-sharing open double hexagonal prisms (Figure 2c, left). With a common bridging OH that may play a critical role during calcination, it was interesting to apply to MIL-34 the same approach that was used for the calcination of $AlPO_4$-14.

The energy minimizations performed here probe the lattice energy and crystal structure of MIL-34 in its calcined form. Indeed, such a computational approach is highly valuable in this typical situation where obtaining a calcined sample of MIL-34 suitable for full characterizations is extremely difficult, especially in the form of a good quality single crystal for structure determination or in the form of a high-quality pure powder (i.e., free of unreacted compounds or extra phases) appropriate for Rietveld refinement or NMR studies.

The single-crystal structure of the as-synthesized MIL-34, $Al_4(PO_4)_4(OH)(C_4H_{10}N)$, was taken as a starting point for our calculations, removing from the original crystal structure the species that are prone to be decomposed upon calcination, i.e., the bridging oxygens, O(4), belonging to OH groups and the CBuA template molecules. These modifications result in a structure in which all four inequivalent Al atoms are in tetrahedral coordination, retaining Al(2) and Al(4) in highly distorted oxygen environments that emanate from the two five-fold-coordinated Al atoms of the as-synthesized structure (Figure 6, left). This model structure was then submitted to constant pressure energy minimization.

In Figure 6 (right), we show the calcined MIL-34 structure as predicted by our energy minimizations. The theoretical atomic positions are given in Table 4, together with the theoretical cell parameters. In terms of topology and connectivity, the calcined MIL-34 structure obviously retains the same architecture as the original model structure. Indeed, the key feature of the simulated calcined structure is its regular zeotype architecture, emanating from the regular and tetrahedral oxygen environments of all Al and P atoms together with the strict alternation of corner-sharing AlO_4 and PO_4 tetrahedra. Typically, Al−O distances are obtained within a more restricted range (1.71−1.77 Å) than that in the as-synthesized structure (1.71−1.97 Å). This generates a regular microporous framework with accessible channels delimited by eight-membered rings. On account of the above findings, the distortions observed in the as-synthesized MIL-34 structure may be considered as a consequence of the Al−OH−Al linkages together with the hydrogen bonds occurring between the template molecules and the inorganic framework.

Another important use of interatomic potentials is that they can test space groups for possible lower symmetry distortions, as found for other AlPOs.[19] The phonon spectrum at the Γ point of the calcined MIL-34 structure was calculated in its original space group *P*-1. The structure was found to be phonon stable in this space group, verifying that the symmetry is at least *P*-1.

Interestingly, our simulations not only predict the crystal structure of the calcined MIL-34 but also anticipate its relative

Table 4. Atomic Coordinates for the Calcined MIL-34 ($AlPO_4$) Structure As Predicted by Our Energy Minimizations Calculations, and As Obtained from the Rietveld Refinement (Italic Characters) in Space Group *P*-1[a]

atom		x	y	z
Al(1)	sim.	0.6931	0.2102	−0.3680
	exp.	*0.695(2)*	*0.211(2)*	*−0.372(1)*
Al(2)	sim.	0.3166	0.1985	−0.1832
	exp.	*0.324(2)*	*0.203(2)*	*−0.180(1)*
Al(3)	sim.	0.9727	0.6761	−0.0581
	exp.	*1.003(2)*	*0.692(2)*	*−0.055(1)*
Al(4)	sim.	0.5202	0.2061	−0.1775
	exp.	*0.508(2)*	*0.205(2)*	*0.181(1)*
P(1)	sim.	−0.4008	0.5106	−0.1849
	exp.	*−0.3914(9)*	*0.507(1)*	*0.178(8)*
P(2)	sim.	−0.3970	−0.0876	−0.3734
	exp.	*−0.403(1)*	*−0.0984(9)*	*−0.371(8)*
P(3)	sim.	−0.2567	−0.0354	−0.0427
	exp.	*−0.2454(1)*	*−0.054(1)*	*−0.048(7)*
P(4)	sim.	−1.0159	0.3292	−0.1842
	exp.	*1.018(1)*	*0.326(1)*	*−0.181(7)*
O(1)[a]	sim.	−0.2909	−0.2062	−0.4953
	exp.	*0.287(4)*	*−0.216(5)*	*−0.491(1)*
O(2)	sim.	0.4319	−0.1956	−0.3096
	exp.	*0.423(5)*	*−0.231(3)*	*−0.324(2)*
O(3)	sim.	−0.8801	−0.2214	−0.2946
	exp.	*0.898(3)*	*0.250(6)*	*−0.298(1)*
O(5)	sim.	−0.3065	−0.0314	−0.3112
	exp.	*0.344(5)*	*0.052(4)*	*−0.309(2)*
O(6)	sim.	−0.5106	−0.4126	−0.2092
	exp.	*−0.492(4)*	*0.407(3)*	*0.214(3)*
O(7)	sim.	−0.4900	−0.6373	−0.1380
	exp.	*−0.494(3)*	*0.633(4)*	*0.140(3)*
O(8)	sim.	−0.5601	−0.0179	−0.3816
	exp.	*0.566(2)*	*0.019(4)*	*−0.370(3)*
O(9)	sim.	−0.3629	−0.6104	−0.2976
	exp.	*−0.375(5)*	*0.616(4)*	*0.295(1)*
O(10)	sim.	−1.0435	−0.5219	−0.1497
	exp.	*−1.042(5)*	*0.517(2)*	*−0.147(3)*
O(11)	sim.	−0.2408	−0.3838	−0.0952
	exp	*0.211(2)*	*0.395(5)*	*0.119(4)*
O(12)	sim.	−1.1694	−0.2886	−0.2073
	exp.	*1.174(4)*	*0.292(6)*	*−0.203(3)*
O(13)	sim.	−0.3286	−0.1730	−0.1060
	exp.	*0.342(4)*	*−0.169(4)*	*−0.101(3)*
O(14)	sim.	−0.0735	−0.1261	−0.0658
	exp.	*0.064(1)*	*−0.148(4)*	*−0.099(3)*
O(15)	sim.	−0.2886	−0.1137	−0.0814
	exp.	*0.273(5)*	*0.087(5)*	*−0.094(3)*
O(16)	sim.	−0.3362	−0.0423	−0.0870
	exp.	*0.328(4)*	*0.030(5)*	*0.081(1)*
O(17)	sim.	−0.9646	−0.2867	−0.0852
	exp.	*0.959(5)*	*0.254(4)*	*−0.095(2)*

[a] See text for details on cell parameters. [b] The numbering of atoms was taken identical to that of the original as-synthesized MIL-34 structure, therefore showing the elimination of O(4) atoms corresponding to hydroxy groups.

stability upon template extraction. Our initial model of calcined MIL-34, starting with highly distorted environments for Al atoms (Figure 6, left) and an initial lattice energy of −12479.22 kJ mol^{-1} per tetrahedral unit, converged rapidly toward the structure in which all Al atoms are in a regular tetrahedral environment, with a final lattice energy of −12922.57 kJ mol^{-1} per tetrahedral unit (Figure 6, right). For comparison, this gives the calcined MIL-34 structure stability similar to that of $AlPO_4$-14 (−12924.9 kJ mol^{-1})[10] but 13.8 kJ mol^{-1} less stable than α-berlinite per T site. For further comparison, the work of Gale and Henson[16] demonstrates that the purest AlPOs are between 4 and 13 kJ mol^{-1} less stable than the thermodynamically favored polymorph under ambient conditions, making MIL-34 a relatively unstable structure, similar to $AlPO_4$-14.

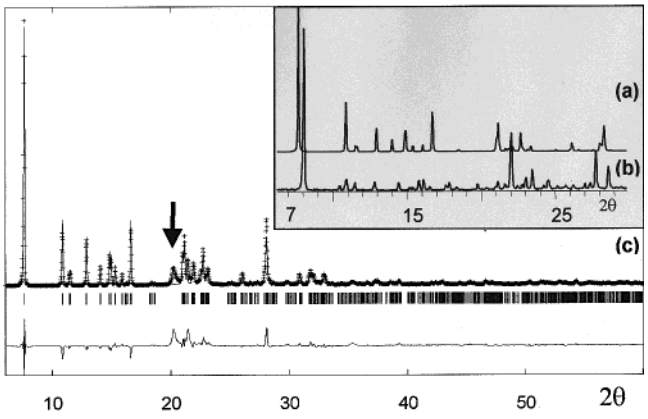

Figure 7. (a) Simulated X-ray powder pattern of the model calcined MIL-34. **(b)** Experimental X-ray powder pattern of as-synthesized MIL-34. **(c)** Rietveld plot for calcined MIL-34 showing the observed data (crosses), the calculated pattern (solid line); tick marks show the Bragg peaks positions; the lower curve is a plot of the difference (observed minus calculated). Additional phases are present. The highest line of the main impurity is shown by a black arrow.

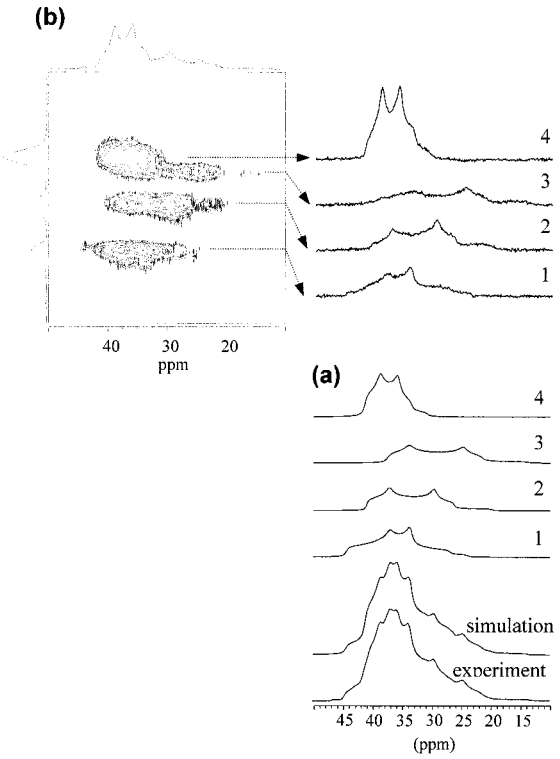

Figure 8. ^{27}Al NMR spectra of calcined MIL-34. **(a)** MAS spectrum. Components: (1) $\delta_{iso} = 44.9$ ppm, $\nu_Q = 705$ kHz ($C_Q = 4.7$ MHz), $\eta_Q = 0.67$; (2) $\delta_{iso} = 42.7$ ppm, $\nu_Q = 760$ kHz ($C_Q = 5.1$ MHz), $\eta_Q = 0.3$; (3) $\delta_{iso} = 39.6$ ppm, $\nu_Q = 810$ kHz ($C_Q = 5.4$ MHz), $\eta_Q = 0.25$; (4) $\delta_{iso} = 41.9$ ppm, $\nu_Q = 525$ kHz ($C_Q = 3.5$ MHz), $\eta_Q = 0.43$; integration 0.28:0.23:0.21:0.27. **(b)** 3QMAS spectrum.

Calcined MIL-34: Crystallographic Findings and NMR Corroborations. To further evaluate the validity of our anticipated model for the calcined MIL-34, we simulated its corresponding X-ray diffraction pattern. It is shown in Figure 7a, together with an experimental pattern of the as-synthesized MIL-34 (Figure 7b), for illustrating the drastic changes in the diffraction features occurring upon calcination. Indeed, when compared to the experimental powder pattern of a calcined MIL-34 sample (Figure 7c), our simulated pattern obtained from our

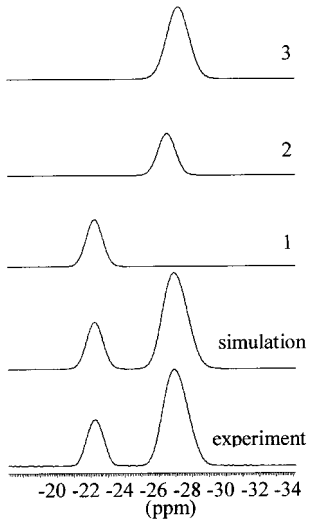

Figure 9. ^{31}P NMR MAS spectrum of calcined MIL-34. (1) $\delta_{iso} = -23.1$ ppm, LW = 230 Hz; (2) $\delta_{iso} = -27.4$ ppm, LW = 246 Hz; (3) $\delta_{iso} = -28.1$ ppm, LW = 311 Hz; integration 0.25:0.24:0.51.

model structure captures the experimental diffraction features remarkably well.

In view of the above agreement, a Rietveld refinement was finally performed on the X-ray powder pattern of the calcined MIL-34 sample, using the theoretical structure obtained from our energy minimizations as a starting model. Soft constraints had to be introduced [d(Al−O) = 1.73(2) Å and d(P−O) = 1.52(1) Å] due to the limited number of reflections compared to that of structural parameters and the presence of impurities. The final fit obtained between calculated and observed patterns shown in Figure 7c converged to $R_P = 0.176$ and $R_F = 0.111$. It involved the following parameters: 72 atomic coordinates, 1 scale factor, 1 zero point and 6 cell parameters, 3 half-width parameters, 4 line asymmetry parameters, 2 variables for the angular variation η, and 6 polynomial background coefficients. The low quality of the Rietveld refinement could be explained by the presence of additional phases (main line shown with an arrow), which probably affects integrated intensities of the calcined MIL-34 phase.

Moreover, indexing of the 20 first lines of this powder pattern [except for the large diffraction line at 20.130° (2θ)] leads to a triclinic solution very similar to that previously obtained by our simulations, with cell parameters as follows: $a = 8.784$ (6) Å, $b = 8.784$ (6) Å, $c = 12.850(6)$ Å, $\alpha = 110.43(4)°$, $\beta = 98.50(5)°$, $\gamma = 104.92(4)°$ and satisfactory figures of merit [$M_{20} = 29$, $F_{20} = 64(0.0082; 38)$].

Additionally, NMR spectra of ^{27}Al (Figure 8, MAS (a), 3QMAS (b)) and ^{31}P (Figure 9, MAS) were collected on the calcined compound. The calcined phase rehydrates very quickly. For different increasing waiting times, between pulling the sample out of the oven and acquisition of the MAS spectrum, a subspectrum (not shown) increases due to rehydration. The anhydrous calcined phase spectra obtained by quickly filling the rotor with the MIL-34 still hot from the drying oven are displayed in Figures 8 and 9. The ^{27}Al calcined spectrum, Figure 8a, contains four equally populated tetrahedral sites, in full agreement with the MIL-34 modeled structure. A full analysis of the 3QMAS and MAS spectra will be subsequently described in a detailed analysis of the ^{27}Al NMR.[26] The ^{31}P spectrum of Figure 9 exhibits three lines in a 1:1:2 ratio, the two last being hardly resolved. Though three inequivalent sites lines are strongly overlapping, the spectrum confirms four inequivalent sites of the simulated and refined structure.

These comparisons unambiguously establish that our lattice energy minimizations yield a valid description of the calcined MIL-34 structure, directly usable as an initial model for crystal structure determination.

Further Characterizations. A sample of calcined MIL-34 was further studied using thermogravimetric analysis and BET surface area measurements in order to characterize the porosity of this new zeotype structure, namely $AlPO_4$. The TGA (Figure 10a) from ambient temperature to 150 °C shows a loss of 12.6% which corresponds to 3.4 water molecules per Al_4P_4 unit, or an average of 6.8 water molecules per $4^8 6^2 8^6$ cage. When the sample was cooled to ambient temperature, the weight of the sample increased back to its initial value, showing that the hydration/dehydration process is completely reversible and that the calcined MIL-34 may be considered as a relatively hygroscopic material. Preliminary NMR measurements on the calcined MIL-34 sample suggest that reversible modifications of the aluminum atoms' coordination occur upon rehydration. The BET surface area and pore structure of the calcined sample activated at 200 °C for 12 h were studied. A typical type-1 isotherm was found (Figure 10b) and yielded a BET surface area of 271 $m^2 \cdot g^{-1}$.

Conclusions

The synthesis and structural characterization of MIL-34 highlight a new strategy in materials elaboration. Once the crystal structure of the as-synthesized MIL-34 ($Al_4(PO_4)_4OH \cdot C_4H_{10}N$) was determined, the calcined template-free structure, namely $AlPO_4$, could be anticipated using appropriate interatomic potentials. The reliability of the simulation allowed us to perform a Rietveld refinement of the powder pattern of the calcined phase. Indeed, this synthesis/simulation/structure sequence starting from the as-synthesized structure up to the calcined stable microporous material is the key feature of our approach. It articulates chemical prediction of the possible

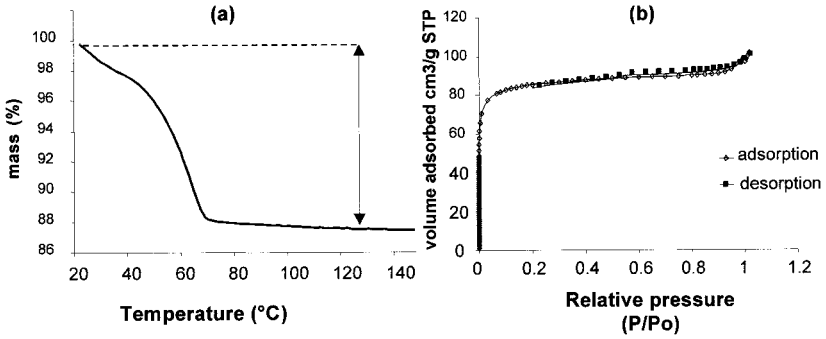

Figure 10. (a) Thermogravimetry analysis of the calcined MIL-34 sample. (b) BET isotherm of the calcined MIL-34 sample.

calcined network from the as-synthesized material and provides the starting point of a Rietveld refinement. The challenge now is to harness the power of this sequence in the systematic investigation of other open-framework materials of interest, where the removal of the template agents from the as-synthesized structures would lead to energetically and thermally stable microporous structures. In this perspective, we are currently working on the extension of interatomic potentials to gallophosphates[27] together with the anticipation of the energetics and structures of a whole series of open-framework GaPOs upon calcination,[28] conveying both dehydroxylation and dehydrofluorination processes. Such developments integrated in this synthesis/simulation/structure sequence open the possibility of tackling two large families of compounds such as aluminophosphates and gallophosphates.

Acknowledgment. The authors are grateful to Dr. Daniel Louer and Gérard Marsolier (L.C.S.I.M., Université de Rennes I, France) for their help in the X-ray data collection of the calcined MIL-34 sample. Stefan Steurnagel from Bruker Rheinstetten is thanked for providing access to the AMX 800 and Zhehong Gan for running the STMAS spectrum (not shown in this paper) on as-synthesized MIL-34. We thank Julian Gale (Imperial College, London) for useful assistance and discussions concerning the use of GULP software.

Supporting Information Available: Selected bond distances and angles for the as-synthesized templated MIL-34 obtained from the single-crystal refinement (PDF). This material is available free of charge via the Internet at http://pubs.acs.org.

JA010575B

(27) Girard, S.; Gale, J. D.; Mellot-Draznieks, C.; Férey G. *Chem. Mater*. **2001**, in press.

(28) Girard, S.; Gale, J. D.; Mellot-Draznieks, C.; Férey G., to be submitted, 2001.